MODEL-DRIVEN ASSESSMENT OF SPACE WEATHER IMPACT LEVELS ON THE TRAJECTORY OF FLOATING DEBRIS IN LOW EARTH ORBIT

Victor U. J. Nwankwo, Jens Berdermann, Frank Heymann, Timothy N. Kodikara and Isabel Fernandez-Gomez

Institute for Solar-Terrestrial Physics, German Aerospace Center (DLR), Neustrelitz (Germany), Email: victor.nwankwo@dle.de

ABSTRACT

Space weather exacerbates the problem of atmospheric drag effect on low Earth orbit (LEO) objects and consequently influence orbital debris population. The severity of impact may vary from object-to-object, depending on their altitude, attitude, ballistic parameters and/or operational dynamics at the time/duration of space weather event. In this paper, we investigate the impact of space weather on floating catalogued debris in LEO during the 25th solar cycle. We model the evolution of orbital decay of the objects (due to space weather-enhanced atmospheric drag) as a function of predicted and observed solar activity indices. We also perform model-driven assessment of the influence of ballistic and attitude variability on the objects' aerodynamic drag. Using the results from ephemeris data-assisted calibrated (EDAC) simulation obtained for various regimes, we provide space situational awareness (SSA) of the objects that are resourceful for the development of relevant concepts for orbital sustainability. Thus, we demonstrate the vital role of the capability to understand and monitor the constantly changing space environment in space sustainability effort.

Keywords: Atmospheric drag; Low Earth orbit; ephemeris data-assisted calibrated; orbit decay rate; space weather

1 INTRODUCTION

Scientifically equipped space-based assets have over the years delivered huge social, scientific, strategic and economic benefits to humanity and practically all sectors of human endeavour throughout the globe. Despite the attendant or perceived challenges, space exploration has enabled ground-breaking and insightful discoveries and provided the foundation for many science and technology-based innovations that are improving societal standard of living. The huge benefits currently being derived from space-based technology (motivating the need to accommodate new opportunities), coupled with global explosion in the commercialisation and militarisation of low-Earth orbit (LEO) will continue drive the launch of more satellites into orbit (see Fig 1, depicting the growth of artificial objects in space since 1957). A chart from NASA Orbital Debris Program Office (ODPO) revealed that satellites in orbit increased from 2063 to 4600 between 2019 and 2021 (see, Fig 1 in [1]). This is a sharp contrast to the number of launches in predated period and a scenario that can potentially lead two important (but opposite) implications to the peaceful and sustainable use of the near-Earth space environment. On a positive note, the increasing number of space-based assets will continue fuelling future discoveries, addressing global challenges in space and on Earth (through the use of innovative technology), creating global partnerships (by sharing challenging and peaceful goals), inspiring society and individual efforts and enabling economic expansion and new business opportunities [2]. On the other hand, the scenario can lead to space congestion and consequently influence the generation of more debris through the so-called 'domino effect'. The traffic condition in LEO is already reaching a worrisome state where space debris (consisting of remnants of on-orbit collisions, exploded spacecraft, defunct satellites, rocket bodies, breakup fragments and mission-related junks) now outnumber active space assets [1].

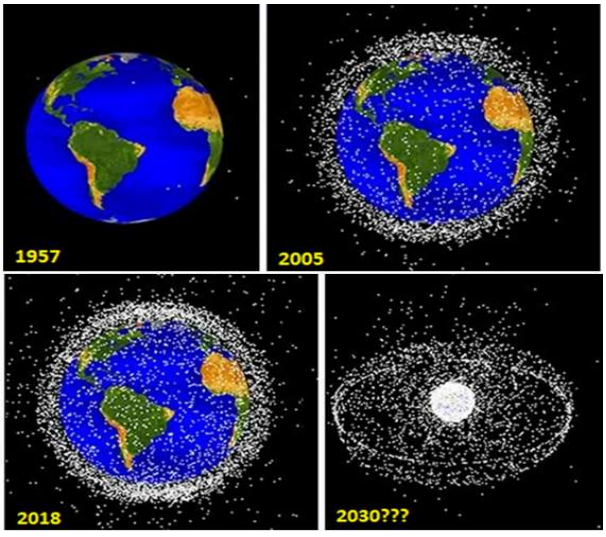

Figure 1. Depiction of the growth of artificial objects in space since the launch of the first satellite in orbit (adopted from https://www.secretsofuniverse.in/space-debris-problem/).

Debris population (if not controlled) can increase the risk and cost of space operation, pose significant risk to both manned (e.g., ISS) and unmanned spacecrafts, as well as life and infrastructure on Earth [3]. Consequently, a risk-free utilisation and sustainability of the space is fast becoming unrealistic by the day. Space weather condition makes the risk even more worrisome. It can drive enhanced atmospheric drag and cause accelerated orbital decay for LEO objects (among other impacts). This scenario that can influence orbital debris population, especially at this period of approaching solar cycle peak. The recent SpaceX satellites incident attest to space weather exacerbation of the problem of atmospheric drag and consequent influence on debris population. On 3 February 2022, 49 Starlink satellites of SpaceX were launched onboard Falcon 9 rocket to LEO. 38 of the satellites were unfortunately destroyed by geomagnetic storms-driven drag enhancement before they were lifted to a higher Earth orbit (Dang et al., 2022[4]; Berger et al., 2023[5]). Atmospheric drag force can also increase the risk of spacecraft collisions due to the increased margins of error in spacecraft positioning e.g., 2009 Iridium - Cosmos collision [6]. However, the severity of such space weather impact may vary from object-to-object, depending on their altitude, attitude, ballistic parameters and/or operational dynamics at the time or duration of energetic solar activity.

The rising threat of space debris necessitates urgent measures towards mitigation of its production and the development of the capabilities to remove existing debris for space and/or orbital sustainability [7]. Most sustainability effort focuses on one or a combination of space situational awareness (SSA) programmes, on-orbit servicing (OOS), active debris removal (ADR) and on-orbit assembly (OOA). Some attempts in this regards include LARAMOTIONS, e.Deorbit, DEOS, MEV-1 and MEV-2, ELSA-d mission, Clearspace-1 and OSAM-1 [1,8-14]. Space debris is a global problem that requires an urgent global solution. Therefore, 'it is in the interest of all nations to collectively resolve the problem of space debris, which can adversely affects all satellites in orbit without discrimination' [3]. As part of an effort to increase sustainability and circular economy in Earth orbit, the German Aerospace Centre (DLR) is synergistically combining cross-program competencies from space, security and aeronautics to pursue a profound view of the space ecosystem to be able to address such [sustainability] goal through short-, medium- and long-term achievable goals of DLR 'Impulsprojekt Orbitale Nachhaltigkeit' (ION).

The short-term goal of the project [ION] pictures a hypothetical debris removal mission that consists of a robotic and satellite technologies for rendezvous and subsequent capture and removal of space debris objects [1]. The results presented in this paper can be categorized under the work scope that provides SSA through technologies for the identification and characterisation of target debris (from ground and space) and modelling their response to atmospheric drag force (in relation to solar activity) for the purpose of the mission planning. Having provided a detailed background of our accomplished drag model (combined with high-fidelity atmospheric specification) in [1], we now present a summarised result of modelling long-term evolution of orbital decay of selected [catalogued] LEO objects (as a function of predicted and observed solar activity indices) during 2023-2024. Subsequently, we perform a detailed model-driven assessment of space weather impact levels on the trajectory of the targets, on the basis of their individual orbital and ballistic parameters.

2 DATA, METHOD AND SCOPE

The formulation of our drag model is based on well-known theoretical framework that is detailed in [1]. We used the Runge-Kutta Fourth Order numerical integration method in a spherical coordinate system for the orbit propagation. The orbital decay was determined as a consequence of changes in the radial distance, r, and the azimuthal angle, Ø, through the following set of coupled equations [1,6]:

1. $\dot{v}_r = -\dot{\emptyset}^{\frac{1}{2}} r^2 \rho \left(\frac{A_s C_d}{m_s}\right)$
2. $\dot{r} = v_r$
3. $\ddot{\emptyset} = -\frac{1}{2} r \rho \dot{\emptyset}^2 \left(\frac{A_s C_d}{m_s}\right)$
4. $\dot{\emptyset} = \frac{v_\emptyset}{r}$

where v_r and $v_\emptyset$ are the radial and tangential velocity components, $\dot{v}_r$ and $\ddot{\emptyset}$ are the radial and azimuthal acceleration, related to the decay rate of semimajor axis and the perturbing acceleration, respectively, as described in equation 3 and 11 of [1]. r is the instantaneous radius of the orbit, ρ is the atmospheric density, A_s, m_s, and C_d are the object's projected area, mass and drag coefficient, respectively.

We selected a list of four catalogued objects for the present work, whose portrait are shown in Fig 2 and their orbital and ballistic parameters provided in Table 1. The m_s and A_s of the objects were obtained from ESA's DISCOSWeb, the apogee, perigee and mean heights, eccentricity (e) and inclination (i) from reliable tracking platforms (e.g., In-the-sky.org/ and N2YO.com). e can also be calculated from equation 9 of [1]. The C_d were assumed based on the recommendations in [15-16]. For this model, the altitude-dependent ρ is obtained from the Naval Research Laboratory Mass Spectrometry and Incoherent Scatter Extended 2000 (NRLMSISE-00) empirical atmospheric model [17].

Figure 2. Portrait of catalogued LEO objects selected for the study [courtesy: commons.wikimedia.org (ERS-2), space.skyrocket.de (Helios-1B) www.eoportal.org (ASAP-S and SPOT-5].

Table 1: The orbital and ballistic parameters of selected objects [1].

	LEO Object	h_m (km)	m (kg)	A (m^2)	Cd	B (m^2/kg)	Ecce., e	Incl., i
1	1995-021A ERS-2	489.86	2494	15.593	2.100	0.013132	0.00047678	98.524°
2	2011-076G ASAP-S	579.88	624	1.5079	2.408	0.005819	0.00045203	98.100°
3	1999-064A HELIOS-1B	626.98	2544	9.273	2.200	0.008019	0.00005410	98.271°
4	2002-021A SPOT-5	724.93	3000	26.052	2.408	0.020911	0.00662587	98.122°

We have monitored the mean height of these objects since January 2023 and thus provide the analysis of space weather influence on the objects for the period of January 2023 to June 2024. To describe the space weather condition during the interval we show solar activity indices for the period, represented by solar radio flux (F10.7) and geomagnetic A_p indices shown in Fig 3. These are the main solar-geomagnetic parameters used as input to obtain the thermospheric density profile for the path through which the objects traversed. F10.7 is often used as a proxy for upper atmospheric heating from solar extreme ultraviolet (EUV) radiation, while A_p represents an estimate of additional Joule heating associated with geomagnetic activity. The moving average of F10.7 over three solar rotations (81 days) was also used to represent a slowly varying component of solar radiation (see, [1] and references therein).

The simulation and/or modelling of a long-term drag impact is challenging (when compared to short-term scenario) and, therefore, requires a framework that is rooted in sound theoretical background [1]. To this end, we employ the ephemeris data-assisted calibration (EDAC) method, which involved the introduction of theory-based indices and/or conditions that minimises the gap between simulated and actual object ephemeris (e.g., spacecraft position, r). Applying the EDAC component to the semimajor axis decay rate (which is a form of equation 3), yields a modulated flightpath modeled as [1]:

5. $\frac{da}{dt} = -\frac{a^2 \rho A C_d}{m_s} \sqrt{\frac{GM_e}{a^3}} \; [\boldsymbol{r}_{mod}]$
6. $\boldsymbol{r}_{mod} = \frac{\Delta r_e}{\Delta r_s}$

where $\Delta r_e = r_{te} - r_{ep}$ is the difference of the actual mean position, r or a (based on ephemeris data), at time t (rt) and the epoch (rep), and $\Delta r_s = r_{ts} - r_{ep}$ is the difference of the simulated mean r or a, at time t (rt) and the epoch (rep).

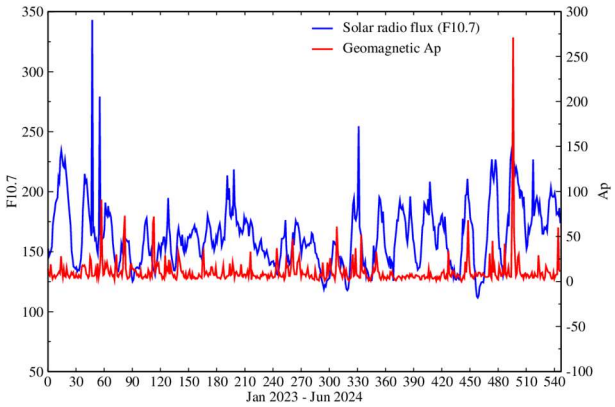

Figure 3. Solar activity indices (F10.7 and A_p) during the interval objects were monitored - January 2023 to June 2024.

Using the EDAC method, we simulated the long-term evolution of orbital decay of the four objects (due to space weather-enhanced atmospheric drag) as a function of predicted and observed solar indices during the time interval of January - June 2023 and January - June 2024. The results of the simulation were presented in detail in [1]. However, in order to lay the foundation of the main goal of this paper we hereby present the abridged form of the results and then a perform more detailed assessment of space weather impact levels on the trajectory of the targets.

3 RESULTS AND DISCUSSION

3.1 Modeling long-term atmospheric drag impact

Figure 4 show the plot of the Actual mean height (h-ACT), simulated mean height as a function of predicted (h-PSI) and observed (h-OSI) solar indices and their corresponding orbit decay rates, ODR (ODR-ACT, ODR-PSI and ODR-OSI) during 1 January to 30 June 2023. The initial height of the objects (ERS-2, ASAP-S, HELIOS-1B and SPOT-5) on 1 January (2023) are 488.53, 579.62, 626.94 356 and 724.93 km, respectively (see, broken blue plot). By the end of June, the objects decayed (due to atmospheric drag influence) to the respective heights of 453.18 (at the 357 end of May), 571.47, 625.16 and 724.44 km on 30 June 2023. Their respective total [orbital] decay (TOD-ACT) during this interval (Jan-Jun) are 35.35, 8.15, 1.78 and 0.49 km. The

simulated results in the predicted solar activity regime (h-PSI) produced mean heights of 457.10, 572.51, 625.39 and 724.41 361 km, respectively, at the end of June, while the simulated mean heights in the observed solar activity regime (h-OSI), are respectively 451.82, 570.98, 625.11 and 724.32 km. when compared with h-ACT (on 1 January), the respective total decay in PSI regime (TOD-PSI) are 31.43, 7.11, 362 1.55 and 0.52 km), while the total decay in OSI regime (TOD-OSI) are 36.71, 8.64, 1.83 and 0.61 km, respectively. The simulated TOD-OSI of the objects for this interval are slightly higher than the TOD-ACT by 1.36, 0.49, 0.05 and 0.12 km, respectively, while the TOD-PSI are -3.92, -1.04, -0.23 and 0.03 km, respectively.

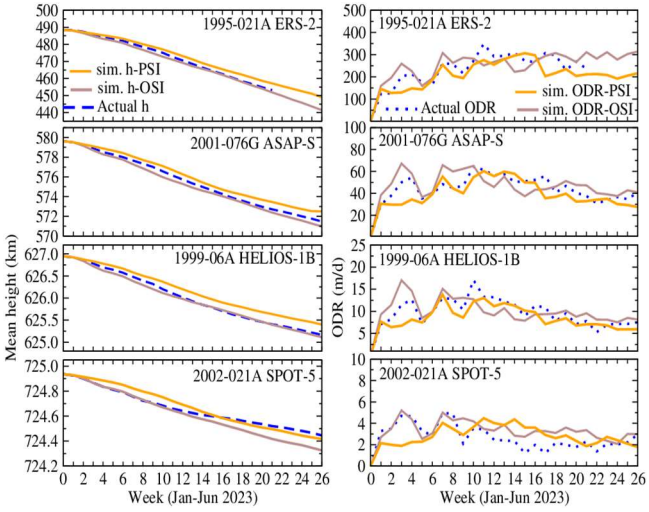

Figure 4. Objects' actual weekly mean height (h), simulated mean height as a function of predicted solar indices (h-PSI) and observed solar indices (h-OSI) and their corresponding orbit decay rates (Actual ODR, ODR-PSI and ODR-OSI) during 1 January to 30 June 2023. The broken blue line represents the Actual h and ODR. The brown line represents h-OSI and ODR-OSI and the orange line represents h-PSI and ODR-PSI [1].

Solar activity continued to increase significantly since 2023 and currently approaching the peak of its 25th cycle (expected before the end of 2025). To underscore the effect of the heightened solar cycle relative to a less solar intense regime during Jan-Jun 2023 (from the standpoint of atmospheric drag), we now extend this investigation to Jan-June 2024 (an interval of more intense solar activity). In Fig 5 show plot of 3 (of the 4) objects' (ASAP-S, HELIOS-1B and SPOT-5) actual height (h-ACT) and the simulated mean height as a function of observed solar indices (h-OSI) and their corresponding orbit decay rates, ODRs (ODR-ACT and ODR-OSI) during 1 January to 30 June 2024. ERS-2 re-entered the Earth's atmosphere on 21 February 2024 and, therefore not included in the analysis for this interval. The objects' initial h-ACT on 1 January 2024 are 564.61, 624.94 and 723.17 km, respectively, which decayed to the respective heights of 556.09, 622.38 and 721.95 km by 30 June 2024. Their respective TOD-ACT during the interval are 8.52, 2.56 and 1.22 km. The objects' simulated h-OSI at the end of June 2024 are 555.38, 622.18 and 721.90 km, respectively, corresponding to respective TOD-OSI of 9.23, 2.76 and 1.27 km.

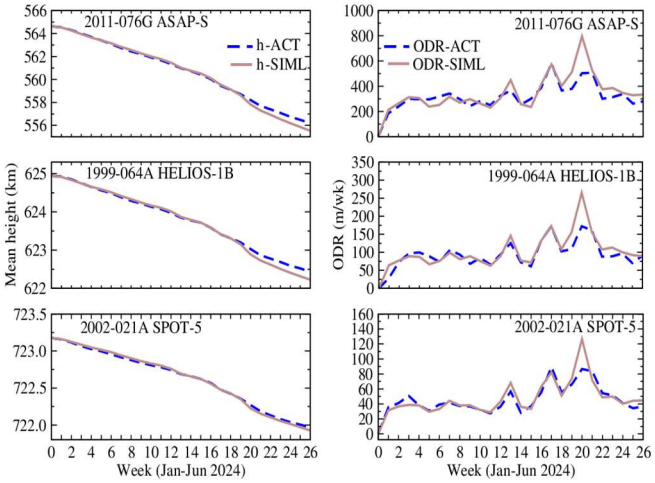

Figure 5. Objects' weekly h-ACT, h-OSI and the corresponding ODR-ACT and ODR-OSI during 1 January to 30 June 2024. The broken blue line represents ODR-ACT/ODR-ACT and the brown line represents h-OSI/ODR-OSI [1].

Figure 6 show the 7-day mean ODR of the LEO objects compared with solar activity indices (A_p, F10.7 and sun spot number (SSN)) during January 2023 to June 2024. It is instructive to see that the ODR-ACT (calculated from the equation of the decay rate of the semimajor axis (da/dt)) are consistent with variations in solar-geomagnetic indices during the entire period; Jan 2023-Jun 2024 [1]. Also, large objects ODR appear to correlate well with elevated F10.7 and/or Ap.

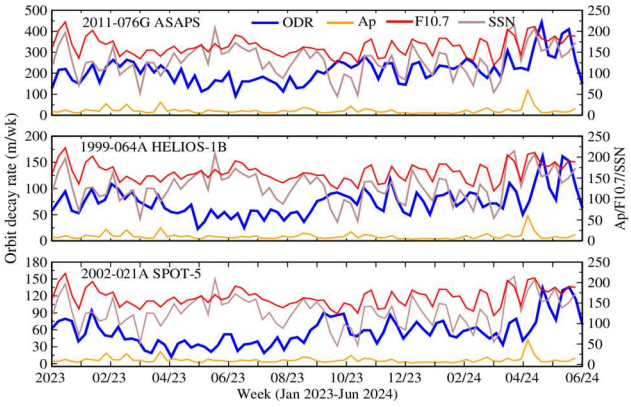

Figure 6. 7-day mean ODR of the LEO objects compared with solar activity indices (A_p, F10.7 and sun spot number (SSN)) during January 2023 to June 2024 [1].

Considering the values of TOD-ACT and TOD-OSI in the foregoing analysis, the standard deviations (σ) of their TODs are ±0.96166522, ±0.34648232, ±0.03535534 and

±0.08485281 km, respectively, in Jan-Jun 2023 and ±0.50204581, ±0.14142136, and ±0.03535534 km, respectively, in Jan-Jun 2024. This outcome shows that the EDAC simulated long-term evolution of atmospheric drag effect on the objects in OSI regime are consistency with the orbital history of the LEO objects. Against this credible background, we now perform a model-driven assessment of space weather impact levels to understand how the trajectory of the targets are affected on the basis of their individual orbital and ballistic parameters at the instant (and duration) of energetic solar activity impact.

3.2 Influence of object's orbital and ballistic parameters on impact level

Most spacecrafts are sometimes required to point to certain direction at intervals, necessitating the change of orientation or attitude [1]. This scenario brings about a change in the object's projected area (A_s) and relatively the exact trajectory dynamics of the objects under investigation. The objects maximum, minimum and mean A_s (hereafter denoted as A_{max}, A_{min} and A_{avg}) and shape are provided in Table 2. When a spacecraft points and sweeps a large area of the thermosphere in motion, it will experience greater drag force (and consequent orbital decay) than the case of a small or reduced surface area (if their m_s is assumed to be constant) s[1]. So far, our simulation utilized the A_{avg} of the objects. To demonstrate the influence of flight associated orbital and ballistic variability (due to change in A_s) on space weather impact level, we now simulate the scenario where the objects fly with A_{max}, A_{min} and A_{avg} during the month of May 2024. The choice of this interval is to accentuate the severe storm event of 10-11 May.

Table 2: The objects shape, maximum, minimum and mean A_s (source: ESA's DISCOSWeb).

	LEO Object	Shape	Max A_s (m^2)	Min A_s (m^2)	Mean A_s (m^2)
1	1995-021A ERS-2	Box + 1 pan	24.872	3.610	15.593
2	2011-076G ASAPS	Cylinder	1.649	1.131	1.508
3	1999-064A HELIOS-1B	Box + 1 pan	11.477	4.000	9.274
4	2002-021A SPOT-5	Box + 1 pan	37.437	9.610	26.052

Figure 7 show the simulated h-OSI and ODR-OSI for the objects' (ASAP-S, HELIOS-1B and SPOT-5) trajectory with A_{max}, A_{min} and A_{avg} during 1-31 May 2024. We assumed that the objects fly with a constant A_s in each case (throughout the entire duration of one month). Although this may not always be the case, the results allow us to assess the level of impact that are associated with the object's range of A_s at any given instant in flight. If the objects orbit or moves with A_{max} (based on the values provided in Table 2) their respective simulated total orbit decay (TOD) and mean ODR (ODR_{avg}) for the month (May 2024) are 2.31 km/86.37 m/day (ASAP-S at h~559.25 km), 0.95 km/24.10 m/day (HELIOS-1B at h~623.50 km) and 0.62 km/36.26 m/day (SPOT-5 at h~722.43). With A_{avg}, the TOD and ODR_{avg} are 2.11 km/78.97 m/day, 0.76 km/17.01 m/day and 0.44 km/29.26 m/day, respectively. The TOD and ODR_{avg} for A_{min} are respectively 1.57 km/59.36 m/day, 0.33/6.397 m/day and 0.16 km/12.59 m/day. A comprehensive summary of this analysis is provided in Table 3.

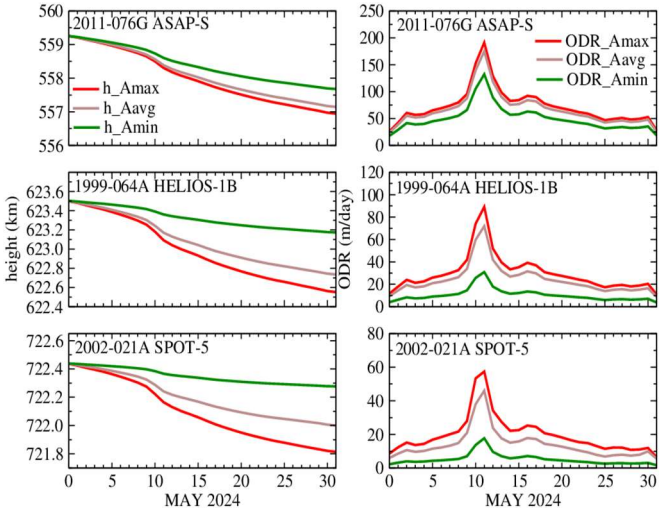

Figure 7. Simulated h-OSI and ODR-OSI for the objects' (ASAP-S, HELIOS-1B and SPOT-5) trajectory with A_{max}, A_{min} and A_{avg} during 1-31 May 2024. The red, brown and green line represent the simulated h/ODR associated with A_{max}, A_{min} and A_{avg}, respectively.

On 10 May 2024 the Earth witnessed the occurrence of a severe geomagnetic storm. Solar activity indices were significant elevated in association with the event (up to Kp~9 [Ap~400] and F10.7~223), which can also be observed in Fig 3. The direct implication of this elevated indices is a strong thermospheric heating by solar extreme ultraviolet (EUV), plus additional heating from geomagnetic perturbations (Nwankwo et al. 2025 and references therein). Consequently, the thermosphere expands, leading to enhanced atmospheric drag on LEO satellites or objects – a signature observed in Fig 7 as accelerated decrease or decay in the objects' h and subsequent increase in ODR between 9th and 12th day of the month (DOM). The severity of impact may vary from object-to-object, depending on their altitude, attitude, ballistic parameters and/or operational dynamics at the time/duration of space weather impact. In the foregoing cases, when the objects fly with A_{max} their associated maximum ODR (ODR_{max}) were up to 191.29, 89.15 and 57.39 m/day, respectively. With A_{avg}, the ODR_{max} were up to 175.23, 71.93 and 46.02 m/day, and up to 132.31, 30.93 and 17.73 m/day, respectively, for A_{min} (also see, Table 3). These ODR_{max} are the corresponding daily values for the peak of the event on 11th DOM. The

specific storm-induced ODR (SSIO) can be calculated from equations 20 and 21 as suggested in Nwankwo et al. (2025). Taking ODR_{avg} (in Table 3) as a baseline for the month, the objects respective SSIO on 11th DOM are 104.92, 65.05 and 21.13 ma/day for A_{max}, 96.26, 54.92 and 16.76 m/day for A_{avg} and 72.95, 24.53 and 5.14 for A_{min}. Similarly, the estimate can be done for selected days within the interval of the storm (e.g., 9th, 10th, 11th or 12th DOM).

Table 3. Space weather impact analysis for 1-31 May 2024. The TOD is the objects total decay for the month, ODR_{avg} is the mean orbit decay rate for the month and ODR_{max} is the maximum decay associated with the severe storm.

Space weather impact-level analysis											
	LEO Object	H (km)	A_{max}			A_{avg}			A_{min}		
			TOD (km)	ODR_{avg} (m/day)	ODR_{max} (m/day)	TOD (km)	ODR_{avg} (m/day)	ODR_{max} (m/day)	TOD (km)	ODR_{avg} (m/day)	ODR_{max} (m/day)
1	ASAP-S	559.25	2.31	86.37	191.29	2.11	78.97	175.23	1.57	59.36	132.31
2	HELIOS1B	623.50	0.95	24.10	89.15	0.76	17.01	71.93	0.33	6.40	30.93
3	SPOT-5	722.43	0.62	36.26	57.39	0.44	29.26	46.02	0.16	12.59	17.73

4 CONCLUSION

In this work, we employed the ephemeris data-assisted calibration (EDAC) simulation method to achieve the modeling of long-term evolution of orbital decay (due to space atmospheric drag) of four catalogued LEO objects as a function of predicted and observed solar indices during January - June 2023 and January - June 2024. Although with slight deviations (that are within tolerable limit), the modeled results show strong consistency with the orbital history of the LEO objects, as well as the signature of the constantly changing space environment (due to solar cycle variation). We further investigated and demonstrated the influence of flight associated orbital and ballistic variabilities on space weather impact levels for the objects. Our results showed (as expected) that impact level varied from object-to-object and significantly depends on the object's altitude, attitude, ballistic parameters (A_s, C_d, m_s) and/or operational dynamics at the time and duration of space weather event. Considering the scenario where the investigated objects (ASAP-S, HELIOS-1B and SPOT-5) fly with a range of projected A_s (A_{max} - A_{min}) during a given interval (1-31 May 2024), the resultant range of ODR (based on monthly mean) could be up to 86-59 m/day (at h~559 km), 24-6 m/day (at h~623 km) and 36-12 m/day (at h~722 km). similarly, the deleterious impact of atmospheric drag on the objects, further exacerbated by the severe geomagnetic storm of May 2024 resulted in significantly increased ODR range of about 191-132, 89-30 and 57-17 m/day, respectively, at the peak of the event on 11 DOM. These findings are resourceful to provision of model-based SSA of LEO objects and also demonstrates the vital role of the capability to understand and monitor the constantly changing space environment in space sustainability effort.

5 ACKNOWLEDGEMENT

This work was supported by the Impulsprojekt Orbitale Nachhaltigkeit (ION) of the German Aerospace Center (DLR).

6 REFERENCES

1. Nwankwo, V.U.J., Berdermann, J., Heymann, F., Kodikara, T.N., Yuan, L., Hoque, M.M., Borries, C. and Fernandez-Gomez I. (2025). *Investigation and modeling of space weather impact on catalogued LEO objects for orbital sustainability in near-Earth space*. J. Space Weather Space Clim. (submitted).

2. International Space Exploration Coordination Group (2013). *Benefits stemming from space exploration*. International Space Exploration Coordination Group (ISECG). https://www.globalspaceexploration.org/?p=497

3. Jakhu, R.S. (2009). *Iridium-Cosmos collision and its implications for space operations*, in: Yearbook on Space Policy 2008/2009, edited by: Schrogl, K.U. et al., Springer, Wien, New York, 254-275. https://link. springer.com/chapter/10.1007/978-3-7091-0318-0_10

4. Dang, T., Li, X., Luo, B., Li, R., Zhang, B., Pham, K., et al. (2022). *Unveiling the space weather during the Starlink satellites destruction event on 4 February 2022*. Space Weather, **20**, e2022SW003152. https: //doi.org/10.1029/2022SW003152.

5. Berger, T.E., Dominique, M., Lucas, G., Pilinski, M., Ray, V., Sewell, R., Sutton, E.K., Thayer, J.P. and Thiemann, E. (2023). *The thermosphere is a drag: The 2022 Starlink incident and the threat of geomagnetic 546 storms to low earth orbit space operations*. Space Weather, **21**(3), p.e2022SW003330. https://doi. 547 org/10.1029/2022SW003330.

6. Nwankwo, V.U.J., W. Denig, S.K. Chakrabarti S.K., Ajakaiye M.P., Fatokun J., Akanni A.W., Raulin J P., Correia E., Enoh J.E. and Anekwe P.I. (2021). *Atmospheric drag effects on modelled low Earth orbit (LEO) satellites during the July 2000 Bastille Day event in contrast to an interval of geomagnetically quiet conditions*. Ann. Geophys., **39**, 397-412.

7. SWF (2018). *Space Sustainability: A practical guide*. Secure World Foundation. www.swfound.org/.

8. Dreyer, H., Scharring, S., Rodmann, J., Riede, W., Bamann, C., Flohrer, T., Setty, S., Di Mira, A. and Cordelli, E. (2021). *Future improvements in conjunction assessment and collision avoidance using a combined laser tracking/nudging network*. https://elib.dlr.de/142042/.

9. Biesbroek, R., Innocenti, L., Wolahan, A. and Serrano, S.M. (2017). *e. Deorbit-ESA's active debris removal mission*. In Proceedings of the 7th European Conference on Space Debris (Vol. 10). ESA Space Debris Office. https://conference.sdo.esoc.esa.int/proceedings/sdc7/ paper/1053/ 551 SDC7-paper1053.pdf.

10. Reintsema, D., Thaeter, J., Rathke, A., Naumann, W., Rank, P. and Sommer, J. (2010). *DEOS - the German robotics approach to secure and de-orbit malfunctioned satellites from low earth orbits*. In Proceedings of the i-SAIRAS (pp. 244-251). Japan: Japan Aerospace Exploration Agency (JAXA). https://api.semanticscholar.org/CorpusID:55274719.

11. Coll, G.T., Webster, G.K., Pankiewicz, O.K., Schlee, K.L., Aranyos, T.J., Nufer, B.M., Fothergill, J.B., Tamasy, G.J., Kandula, M., Felt, A.M. and Hicks, N.G. (2020). *NASA's Exploration and In-Space Services (NExIS) Division OSAM-1 Propellant Transfer Subsystem Progress 2020*. In 2020 AIAA Propulsion and Energy Forum. https://ntrs.nasa.gov/citations/20205004116.

12. Fujii, G., Iizuka, S., Belle, C. and Muktoyuk, M. (2021). The World's first commercial debris removal demonstration mission. https://digitalcommons.usu.edu/cgi/viewcontent.cgi? article=5019&context=smallsat.

13. Biesbroek, R., Aziz, S., Wolahan, A., Cipolla, S.F., Richard-Noca, M. and Piguet, L. (2021). *The clearspace-1 mission: ESA and clearspace team up to remove debris*. In Proc. 8th Eur. Conf. Sp. Debris (pp. 1-3). https://conference.sdo.esoc.esa.int/proceedings/sdc8/ paper/320/SDC8-paper320.pdf.

14. Pyrak, M. and Anderson, J. (2022). *Performance of northrop grumman's mission extension vehicle (mev) rpo imagers at geo*. In Autonomous systems: Sensors, processing and security for ground, air, sea and space vehicles and infrastructure 2022 (Vol. 12115, pp. 64-82). SPIE. https://doi.org/10.1117/12.2631524.

15. Moe, M.M., Wallace, S.D. and Moe, K. (1995). *Recommended drag coefficients for aeronomic satellites*. The Upper Mesosphere and Lower Thermosphere: A Review of Experiment and Theory, **87**, 349-356. https://citeseerx.ist.psu.edu/document?repid=rep1&type=pdf&doi= c4e4e6b250b6a733a717e157897fbb23e84bd1f3.

16. Moe, K., Moe, M.M. and Wallace, S.D. (1998). *Improved satellite drag coefficient calculations from orbital measurements of energy accommodation*. J. Spacecr. Rockets, **35**(3), 266-272. https://doi.org/10. 625 2514/2.3350

17. Picone, J. M., Hedin, A. E., Drob, D. P., & Aikin, A. C. (2002). *NRLMSISE-00 empirical model of the atmosphere: Statistical comparisons and scientific issues*. J Geophys. Res.: Space Physics, **107**(A12), SIA 15. https://doi.org/10.1029/2002JA009430.